

Pentafluoronitrosulfane, SF₅NO₂Norman Lu,^{*,†} Joseph S. Thrasher,[†] Stefan von Ahsen,[‡] Helge Willner,^{*,‡} Drahomir Hnyk,[§] and Heinz Oberhammer^{*,||}

Department of Chemistry, University of Alabama, Tuscaloosa, Alabama 35487,
FB C Anorganische Chemie, Universität Wuppertal, Gausstrasse 20,
D-42119 Wuppertal, Germany, Institute of Inorganic Chemistry, Academy of Sciences,
Cz-25068 Rež, Czech Republic, and Institut für Physikalische und Theoretische Chemie,
Universität Tübingen, D-72076 Tübingen, Germany

Received September 21, 2005

The synthesis of pentafluoronitrosulfane, SF₅NO₂, is accomplished either by reacting N(SF₅)₃ with NO₂ or by the photolysis of a SF₅Br/NO₂ mixture using diazo lamps. The product is purified by treatment with CsF and repeated trap-to-trap condensation. The solid compound melts at −78 °C, and the extrapolated boiling point is 9 °C. SF₅NO₂ is characterized by ¹⁹F, ¹⁵N NMR, IR, Raman, and UV spectroscopy as well as by mass spectrometry. The molecular structure of SF₅NO₂ is determined by gas electron diffraction. The molecule possesses C_{2v} symmetry with the NO₂ group staggering the equatorial S–F bonds and an extremely long 1.903(7) Å S–N bond. Calculated bond enthalpies depend strongly on the computational method: 159 (MP2/6-311G++(3df)) and 87 kJ mol^{−1} (B3LYP/6-311++G-(3df)). The experimental geometry and vibrational spectrum are reproduced reasonably well by quantum chemical calculations.

Introduction

Derivatives of sulfur hexafluoride of the type SF₅–X are of great interest from a chemical and bonding point of view. The kinetically inert and bulky SF₅ group with a highly charged sulfur atom has a strong influence on the S–X bond and on the charge distribution of the substituent X. This has consequences for the stability of the SF₅–X molecules and the synthetic routes. There are numerous SF₅–C, SF₅–N, and SF₅–O compounds that are well known,^{1–4} but the synthesis of SF₅–X compounds, with X being an element of the second or higher period (except for X = SF₅, Cl, or Br) or some simple substituent (e.g., H, I, NO, NO₂, N₃, etc.), has been a challenge for preparative chemists.

Herein we report the first successful preparation of the long sought after pentafluoronitrosulfane, SF₅NO₂, and its unambiguous characterization.

Experimental Section

Synthesis of SF₅NO₂. The synthesis of SF₅NO₂ was carried out by two different methods: (i) by the treatment of N(SF₅)₃⁴ with NO₂ at room temperature and (ii) by the photolysis of a mixture of SF₅Br⁵ and NO₂.

(i) The amine N(SF₅)₃ (0.36 g, 0.90 mmol) and NO₂ (0.12 g, 2.60 mmol) were vacuum transferred at −196 °C into an FEP tube equipped with a metal valve. Subsequently, the reaction vessel was allowed to warm gradually to room temperature, and after 4 h, all N(SF₅)₃ crystals had disappeared. The volatile products were subjected to repeated trap-to-trap condensation in traps held at −105, −130, and −196 °C. A few milligrams of SF₅NO₂ was retained in the trap at −130 °C.

(ii) The compounds SF₅Br (3.9 g, 18.8 mmol) and NO₂ (0.9 g, 19.6 mmol) were transferred into a 4 L Pyrex reactor, which was surrounded by 12 diazo lamps (TL 40 W/03). After 12 h of irradiation, the resulting product mixture was condensed into a 300 mL stainless steel cylinder held at −196 °C. This cylinder was then warmed to the temperature of dry ice, and all of the materials that are volatile at this temperature were vacuum transferred into

* To whom correspondence should be addressed. E-mail: willner@uni-wuppertal.de (H.W.), heinz.oberhammer@uni-tuebingen.de (H.O.), normanlu@ntut.edu.tw (N.L.).

[†] University of Alabama.

[‡] Universität Wuppertal.

[§] Academy of Sciences.

^{||} Universität Tübingen.

(1) Tullock, C. W.; Coffmann, D. D.; Muetterties, E. L. *J. Am. Chem. Soc.* **1964**, *86*, 357.

(2) Senning, A. *Sulfur in Organic and Inorganic Chemistry*; Dekker: New York, 1982; Vol. 4.

(3) *Gmelins Handbuch der Anorganischen Chemie*; Springer-Verlag: Berlin, 1978.

(4) Thrasher, J. S.; Nielson, J. B. *J. Am. Chem. Soc.* **1986**, *108*, 1108.

(5) Winter, R.; Terjeson, R.; Gard, G. L. *J. Fluorine Chem.* **1998**, *89*, 105.

another cylinder containing 400 g of CsF. In this manner, Br_2 , SOF_4 , and SF_4 were removed from the reaction mixture. Subsequently, trap-to-trap condensations through three traps held at -78 , -130 , and -196 °C were carried out to separate SF_5NO_2 from impurities such as FNO and SF_6 . About 90% pure SF_5NO_2 (0.09 g, 0.56 mmol) was obtained in the -130 °C trap with a yield of 3%. Several batches were again purified together by trap-to-trap condensation under IR control. The resulting sample of about 98% purity, with traces of S_2F_{10} and SF_4O , was then used for the following characterization.

Analysis. Volatile materials were manipulated in a glass vacuum line of known volume, equipped with two capacitance pressure gauges (MKS Baratron 221 AHS-1000 and 221 AHS-10 Wilmington, MA), three U-traps, and valves with PTFE stems (Young, London, U.K.). The vacuum line was connected to an IR gas cell (optical path length 200 mm, 0.5-mm-thick silicon windows) in the sample compartment of an FTIR instrument. This arrangement made it possible to follow the improvement in the purification process. The product was stored in glass ampules under liquid nitrogen. The ampules were opened and flame sealed again by means of an ampule key.⁶

(a) NMR Spectroscopy. The ^{19}F , ^{15}N , and ^{14}N NMR spectra were recorded on a Bruker model AM 500 spectrometer at 470.507, 50.677, and 36.127 MHz for ^{19}F , ^{15}N , and ^{14}N nuclei, respectively. The samples were condensed and sealed into glass tubes (4 mm o.d.) on a vacuum line. As the external reference/lock, $\text{CFCl}_3/\text{CD}_2\text{Cl}_2$, $\text{K}^{15}\text{NO}_3/\text{D}_2\text{O}$, and $\text{NH}_4\text{NO}_3/\text{D}_2\text{O}$ (reference peak, NO_3^- , was set at 383 ppm) were used.

(b) Vibrational Spectroscopy. IR spectra of gaseous samples were measured in the range of $4000\text{--}400\text{ cm}^{-1}$ with an FTIR spectrometer (type 400 D, Nicolet, Madison, WI) with an optical resolution of 2 cm^{-1} , and 32 scans were coadded for each spectrum.

Matrix IR spectra of SF_5NO_2 were recorded on a Bruker IFS 66v/s FTIR instrument in reflectance mode using a transfer optic. A DTGS detector and a KBr/Ge beam splitter were used in the $4000\text{--}400\text{ cm}^{-1}$ region. Sixty-four scans were coadded for each spectrum using an apodized resolution of 1 cm^{-1} . Details of the matrix apparatus have been described elsewhere.^{7,8} A small amount of pure SF_5NO_2 (ca. 0.1 mmol) was kept in a small U-trap at -196 °C and mounted in front of the matrix support. The trap was allowed to reach a temperature of -65 °C while a gas stream ($2\text{--}4\text{ mmol h}^{-1}$) of argon or neon was directed over the SF_5NO_2 sample and the resulting gas mixture was quenched on the matrix support at 15 or 6 K, respectively. During matrix deposition, the end of the spray-on nozzle in front of the matrix support was heated to different temperatures.

An FT-Raman spectrum of a solid SF_5NO_2 sample at -196 °C was measured in the region of $3000\text{--}50\text{ cm}^{-1}$ at a resolution of 4 cm^{-1} with an FT-Raman spectrometer (RFS 100/s, Bruker, Germany) by coadding 128 scans and using the 1064 nm excitation line (500 mW) of an Nd:YAG laser. The sample was condensed as a spot on a nickel-plated copper finger kept at -196 °C in high vacuum. The solid sample was then excited with the laser through a quartz window.

(c) UV Spectroscopy. UV spectra of SF_5NO_2 were recorded at room temperature with a Perkin–Elmer Lambda 900 spectrometer with a resolution of 1 nm. Different amounts of the sample were

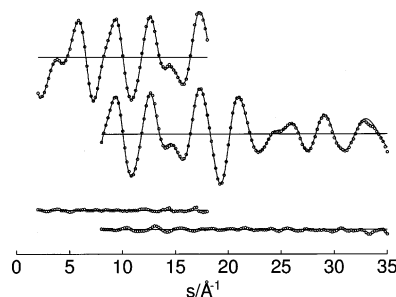


Figure 1. Experimental (•) and calculated (—) molecular intensities for long (above) and short (below) nozzle-to-plate distances and residuals.

transferred into a glass cell of 10 cm optical path length equipped with suprasil windows. The absorption cross sections (on base e) were calculated by means of the equation $\sigma = 31.79TA\rho^{-1}d^{-1}$, where σ is the cross-section in 10^{-20} cm^2 , T is the temperature in K, A is the absorbance, p is the gas pressure in mbar, and d is the optical path length in cm.

(d) Mass Spectrometry. Gas chromatography/mass spectrometry data were obtained using a Hewlett-Packard HP 6890 series gas chromatograph with a series 5973 mass-selective detector. The column was a 6890 GC using a $30\text{ m} \times 0.250\text{ mm}$ HP-1 capillary column with a $0.25\text{ }\mu\text{m}$ stationary-phase film thickness. The flow rate was 1 mL/min and splitless. The electron impact mass spectrum of SF_5NO_2 was obtained at 70 eV. Because SF_5NO_2 is thermally unstable, special conditions were used in an attempt to detect the parent ion and the expected fragmentation pattern. For example, the normal injector temperature of 250 °C and detector temperature of 280 °C were lowered to 48 and 65 °C, respectively. The column temperature was 35 °C. However, no parent ion (SF_5NO_2^+) was observed in the electron impact spectrum even under these conditions.

(e) Vapor Pressure. The vapor pressure of the neat sample was measured by using the above-mentioned vacuum line. The temperature of the sample reservoir was adjusted with a series of ethanol cold baths and measured with a Pt-100 resistance thermometer. Occasionally, the gas phase was checked through its IR spectrum. Very little decomposition ($<1\%$) was detected at temperatures up to -10 °C. Before recording the vapor pressures, we determined the melting point of SF_5NO_2 in the reservoir.

(f) GED Measurements. Electron scattering intensity data for SF_5NO_2 were recorded on Kodak electron image plates using a KDG2-Diffraktograph⁹ at the University of Tübingen, operating at approximately 60 kV, at two nozzle-to-plate distances (25 and 50 cm). The sample was kept at -60 °C, and the inlet nozzle was at room temperature during the experiments. Scattering data for ZnO were recorded simultaneously and used to calibrate the electron wavelength. Data were obtained in digital form using a microdensitometer at the University of Ulm. The photographic plates were analyzed by the usual procedures.¹⁰ Averaged molecular intensities in the s ranges of $2\text{--}18$ and $8\text{--}35\text{ Å}^{-1}$ ($s = (4\pi/\lambda) \sin \theta/2$, λ = electron wavelength, θ = scattering angle) are shown in Figure 1.

(g) Theoretical Calculations. The structure of the title compound was optimized with the MP2 approximation and the B3LYP method using 6-311++G(3df) basis sets. The calculated structure possesses C_{2v} symmetry with the NO_2 group staggering the equatorial S–F bonds. The calculated (MP2) barrier of the four-fold potential function for internal rotation around the S–N bond is 5.4 kJ mol^{-1} .

(6) Gombler, W.; Willner, H. *J. Phys. E: Sci. Instrum.* **1987**, 20, 1286.

(7) Schnöckel, H.; Willner, H. In *Infrared and Raman Spectroscopy: Methods and Applications*; Schrader, B., Ed.; VCH: Weinheim, Germany, 1994; p 297.

(8) Argüello, G. A.; Grothe, H.; Kronberg, M.; Willner, H.; Mack, H.-G. *J. Phys. Chem.* **1995**, 99, 17525.

(9) Oberhammer, H. In *Molecular Structure by Diffraction Methods*; Chemical Society: London, 1976; Vol. 4, p 24.

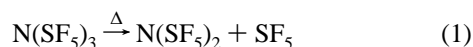
(10) Oberhammer, H.; Gombler, W.; Willner, H. *J. Mol. Struct.* **1981**, 70, 273.

Geometry optimizations with small basis sets (6-31G(d)) predict the S–N and S–F bonds to be too long by up to 0.14 and 0.07 Å, respectively. All of these calculations were performed using the Gaussian 98 package.¹¹ Vibrational amplitudes and vibrational corrections for all interatomic distances were derived from a calculated force field (MP2/6-31G(d)), using the Sipachev method.^{12–14}

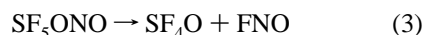
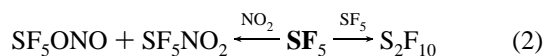
Results and Discussion

Synthesis and Thermal Properties of SF₅NO₂. Two routes to SF₅NO₂ have been found: (i) thermal reaction of N(SF₅)₃ with NO₂ and (ii) photolysis of a SF₅Br/NO₂ mixture.

The compound N(SF₅)₃ slowly decomposes at room temperature,⁴ and the primary step in the decomposition



has been studied through matrix-isolation experiments.¹⁵ The SF₅ radicals can recombine either with each other or with NO₂:



As observed in the reaction of NO₂ with chlorine atoms,¹⁶ O- or N-bonded products SF₅ONO or SF₅NO₂ can be formed. In an attempted synthesis of SF₅ONO by reacting SF₅OCl with ClNO, only the formation of Cl₂, SF₄O, and FNO was found.¹⁷ Hence, SF₅ONO quickly decomposes according to eq 3.

Because SF₅NO₂ also decomposes under the reaction conditions, the yield of the desired product is very low. Furthermore, the difficult multistep synthesis of N(SF₅)₃⁴ precludes a study of its chemistry.

In contrast, starting material SF₅Br⁵ is readily available. Therefore, irradiation of SF₅Br/NO₂ mixtures with diazo lamps ($\lambda_{\text{max}} = 420 \text{ nm}$) has allowed the preparation of gram quantities of the title compound. SF₅Br does not absorb light at 420 nm; hence, excited NO₂ radicals must be involved in the formation of SF₅ radicals. (The threshold for the photodissociation of NO₂ is below 420 nm.) Several subse-

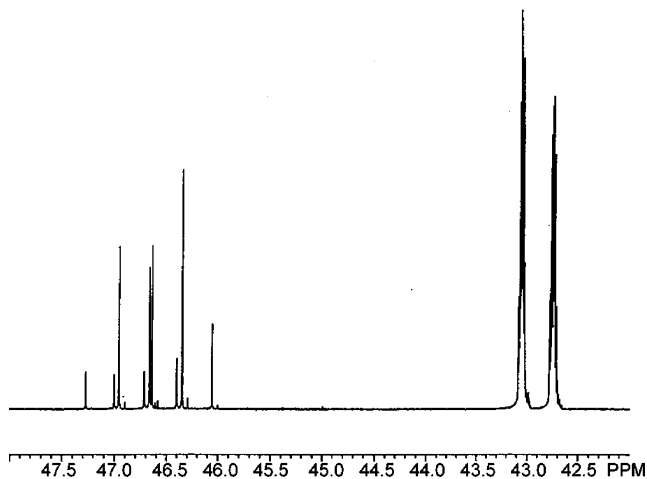
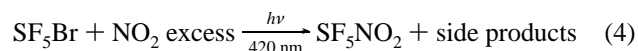


Figure 2. ¹⁹F NMR spectrum of SF₅¹⁵NO₂.

quent reactions of the SF₅ radicals in the reaction mixture lead to SF₅NO₂ and side products S₂F₁₀, SF₆, SF₄, SF₄O, FNO, Br₂, et cetera. The expected product BrNO₂ is not stable under the reaction conditions.¹⁸



The side products of some fluoride ion affinities are absorbed by CsF, and the remaining compounds are separated from SF₅NO₂ by repeated trap-to-trap condensation.

Pure SF₅NO₂ is a colorless gas that decomposes mainly into S₂F₁₀ and NO₂ (and some SF₄O and FNO) at a rate of about 3% per day at room temperature. The white solid melts at –78 °C, and the boiling point amounts to 9 °C by extrapolating the vapor-pressure curve

$$\ln(p/p_o) = -\frac{3788}{T} + 13.33 \quad (5)$$

recorded between –75 and –10 °C.

SF₅NO₂ has been used as a good source of SF₅ radicals.¹⁵ By low-pressure flash thermolysis of SF₅NO₂ with subsequent trapping of the products in inert gas matrixes, mainly SF₅ and NO₂ are detected by IR spectroscopy along with SF₄O, FNO, SF₄, and SF₆.¹⁵

Spectroscopic Properties. (a) NMR Spectra. Figure 2 shows the ¹⁹F NMR spectrum of SF₅¹⁵NO₂ with the typical AB₄ pattern and the splitting of the B₄ signals (F_{eq}) into a doublet due to the ¹⁵N atom. An expansion of equatorial ¹⁹F resonances is depicted in Figure 3. Spectra simulation yielded $\delta(\text{F}_{\text{ax}}) = 46.65$; $\delta(\text{F}_{\text{eq}}) = 42.92$; $^2J(\text{F}_{\text{ax}}\text{F}_{\text{eq}}) = 144.1$; and $^2J(\text{F}^{15}\text{N}) = 11.6 \text{ Hz}$.

The quintet of the ¹⁵N NMR resonance is shown in Figure 4, which also confirms the structure of SF₅¹⁵NO₂ with four equatorial fluorines symmetrically bonded to the S atom. The four equatorial fluorines couple to the ¹⁵N atom but not to the axial fluorine. It is known that the coupling constant of an axial fluorine to a given nucleus is usually 1/10 that of equatorial fluorines to the same nucleus. However, in the

- (11) Frisch, M. J.; Trucks, G. W.; Schlegel, H. B.; Scuseria, G. E.; Robb, M. A.; Cheeseman, J. R.; Zakrzewski, V. G.; Montgomery, J. A., Jr.; Stratmann, R. E.; Burant, J. C.; Dapprich, S.; Millam, J. M.; Daniels, A. D.; Kudin, K. N.; Strain, M. C.; Farkas, O.; Tomasi, J.; Barone, V.; Cossi, M.; Cammi, R.; Mennucci, B.; Pomelli, C.; Adamo, C.; Clifford, S.; Ochterski, J.; Petersson, G. A.; Ayala, P. Y.; Cui, Q.; Morokuma, K.; Malick, D. K.; Rabuck, A. D.; Raghavachari, K.; Foresman, J. B.; Cioslowski, J.; Ortiz, J. V.; Stefanov, B. B.; Liu, G.; Liashenko, A.; Piskorz, P.; Komaromi, I.; Gomperts, R.; Martin, R. L.; Fox, D. J.; Keith, T.; Al-Laham, M. A.; Peng, C. Y.; Nanayakkara, A.; Gonzalez, C.; Challacombe, M.; Gill, P. M. W.; Johnson, B. G.; Chen, W.; Wong, M. W.; Andres, J. L.; Head-Gordon, M.; Replogle, E. S.; Pople, J. A. *Gaussian 98*, revision A.5; Gaussian, Inc.: Pittsburgh, PA, 1998.
- (12) Sipachev, V. A. *J. Mol. Struct. THEOCHEM* **1985**, 121, 143.
- (13) Sipachev, V. A. *Adv. Mol. Struct. Res.* **1999**, 5, 263.
- (14) Sipachev, V. A. *NATO Sci. Ser., Ser. II* **2002**, 68, 73.
- (15) Kronberg, M.; Ahsen, S. v.; Willner, H.; Francisco, J. S. *Angew. Chem., Int. Ed.* **2005**, 44, 253.
- (16) Niki, H.; Maker, P. D.; Savage, P. D.; Breitenbach, L. P. *Chem. Phys. Lett.* **1978**, 59, 78.
- (17) Ulic, S. E.; Willner, H. Unpublished work.

- (18) Scheffler, D.; Grothe, H.; Willner, H.; Frenzel, A.; Zetzsch, C. *Inorg. Chem.* **1997**, 36, 335.

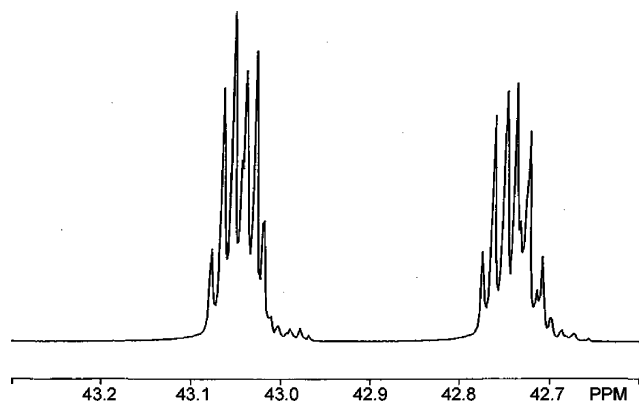


Figure 3. ^{19}F NMR spectrum of $\text{SF}_5^{15}\text{NO}_2$, the expanded B₄ part.

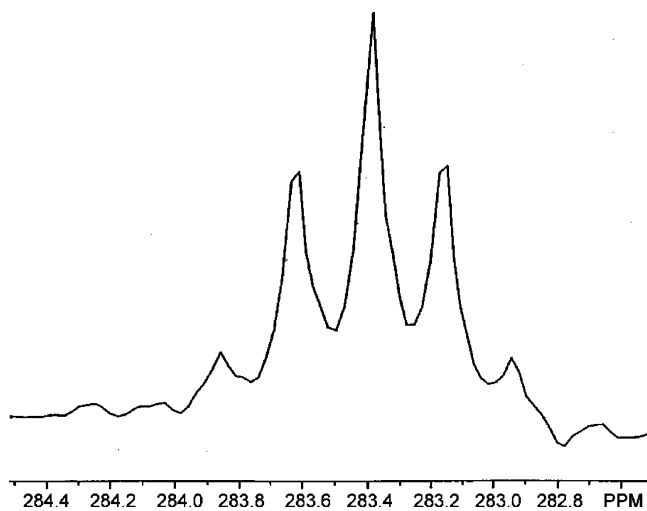


Figure 4. ^{15}N NMR spectrum of $\text{SF}_5^{15}\text{NO}_2$.

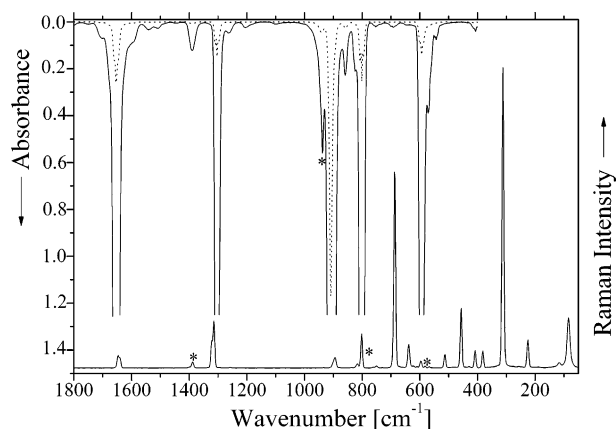


Figure 5. IR spectrum of gaseous SF_5NO_2 (0.6/10.3 mbar, 20 cm optical path length, 23 °C, upper trace) and Raman spectrum of solid SF_5NO_2 at -196 °C (lower trace). Impurities - *.

case of $\text{SF}_5^{15}\text{NO}_2$, coupling between the axial fluorine and the ^{15}N atom was not observed.

(b) Vibrational Spectra. The gas-phase IR and solid-phase Raman spectra of SF_5NO_2 are depicted in Figure 5. All vibrational data observed in the gas phase, in a neon matrix, and for a solid sample are listed in Table 1 and are compared with predicted data from quantum chemical calculations, and a tentative assignment of modes is also given.

The 21 fundamental vibrations of the SF_5NO_2 molecule with the symmetry point group C_{2v} transform as $7a_1$ (IR, Ra

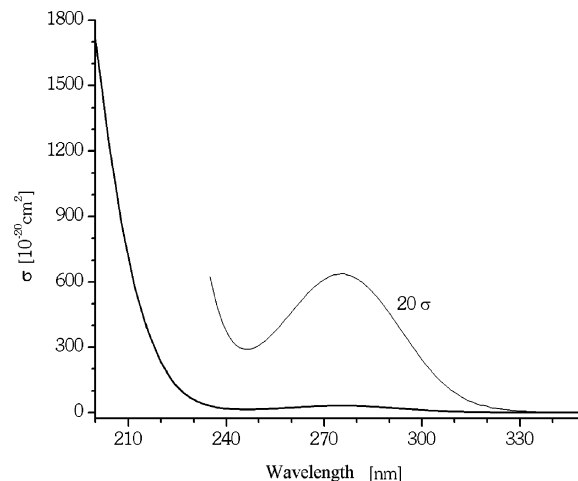


Figure 6. UV spectrum of SF_5NO_2 in the gas phase at 23 °C.

p) + $3a_2$ (Ra dp) + $5b_1$ (IR, Ra dp) + $6b_2$ (IR, Ra dp) vibrations. They can be attributed to 8 stretching, 1 torsional, and 12 deformation modes. Assignment to the relevant symmetry class is assisted by the observed band contours in the gas-phase IR spectrum and isotopic shifts as well as through comparison with characteristic group frequencies in related molecules and predicted band positions and the relative IR and Raman intensities obtained by quantum chemical calculations. Although the band positions (except for $\nu_a \text{NO}_2$) are reproduced reasonably well with the MP2/6-31G(d) method, the IR and Raman band intensities fit better with the B3LYP/6-311G(d) method.

The SF_5NO_2 molecule is a nearly symmetric top rotor; therefore, the a_1 -type bands should exhibit a pronounced PQR band contour. This is true for the gas-phase bands at 1304, 801, and 597 cm^{-1} . The assignment of characteristic NO_2 vibrations $\nu_a = 1653$, $\nu_s = 1304$, and $\delta = 801 \text{ cm}^{-1}$ is confirmed by ^{15}N substitution, which causes the shifts to occur at lower wavenumbers of 36, 16, and 8 cm^{-1} , respectively. The most intense IR band near 910 cm^{-1} in the gas phase is split into several components in the Ne matrix, which are assigned to the SF_{ax} stretching mode and the two components of $\nu_a \text{SF}_{4eq}$. All other bands are more or less coupled, and the description of modes on the basis of the calculated displacement vectors is in part arbitrary.

(c) UV Spectrum. In the UV region, gaseous SF_5NO_2 shows an unstructured absorption at 276 nm and does not absorb the radiation of the diazo lamps used in the synthesis. The absorption may be assigned to the $n \rightarrow \pi^*$ transition of the NO_2 chromophore. Toward shorter wavelengths, there is increased absorption with the maximum below 200 nm. The spectrum is depicted in Figure 6, and absorption cross sections are shown in Table 2.

(d) Mass Spectrum. The 70 eV mass spectrum of SF_5NO_2 shows the following fragment ion pattern, m/z (% ion): 127 (100, SF_5^+), 108 (6.7, SF_4^+), 89 (51, SF_3^+), 81 (1.5, SFNO^+), 70 (12, SF_2^+), 64 (12, SO_2^+), 51 (5.9, SF^+), 46 (69, NO_2^+). Although the molecular ion was missing, the mass spectrum does have fragments of $m/u = 46$ and 127 indicating the presence of NO_2 and SF_5 , respectively. In addition, the peak at $m/z = 81$, which corresponds to SFNO^+ ,

Table 1. Experimental and Calculated Fundamental Wavenumbers and Band Intensities of SF₅NO₂

IR gas	σ^b	IR Ne	I^c	Raman solid	I^d	calcd ^a	I_{IR}^e	I_{Raman}^f	assignm. acc. to C _{2v} symmetry
1653	353	1652	56	1646	w	1893	312	5	ν_{16} b ₂
1304	201	1304	21	1315	m	1314	262	10	ν_1 a ₁
		916	7			948	34	1	ν_2 a ₁
909	1580	910	100	894	w	945	327	3	ν_{17} b ₂
		907				931	384	4	ν_{11} b ₁
801	335	800	26	802	m	793	395	2	ν_3 a ₁
						690	15	<1	ν_{12} b ₁
				687	s	658	3	29	ν_4 a ₁
				638	w	649	0	5	ν_8 a ₂
597	192	594	15	596	vw	580	119	3	ν_5 a ₁
		580	2.8	582	vw	542	4	<1	ν_{18} b ₂
571	31	567	3.9			523	10	<1	ν_{13} b ₁
				513	w	465	<1	2	ν_6 a ₁
				457	m	438	1	8	ν_{19} b ₂
405	4	407	1.3	407	w	373	3	2	ν_{14} b ₁
						362	1	<1	ν_{20} b ₂
						308	0	0	ν_9 a ₂
				312	vs	305	19	22	ν_7 a ₁
				226	w	208	1	2	ν_{15} b ₁
						200	<1	<1	ν_{21} b ₂
						75	0	2	ν_{10} a ₂
									τ N-S

^a MP2/6-31G(d). ^b At band maximum in 10⁻²⁰ cm². ^c Integrated band intensities. ^d Abbreviations for strong, medium, weak, and very weak. ^e km²mol⁻¹ (B3LYP/6-311G(d)). ^f Å⁴amu⁻¹ (B3LYP/6-311G(d)).

Table 2. UV Absorption Cross Sections of SF₅NO₂ in the Gas Phase

λ (nm)	σ (10 ⁻²⁰ cm ²)	λ (nm)	σ (10 ⁻²⁰ cm ²)	λ (nm)	σ (10 ⁻²⁰ cm ²)
200	1708	250	15	300	12
205	1147	255	19	305	7.9
210	715	260	23	310	4.7
215	420	265	28	315	2.6
220	230	270	31	320	1.5
225	119	276 ^a	32	325	0.8
230	60	280	31	330	0.4
235	31	285	28	335	0.2
240	19	290	23	340	0.1
245	15	295	17		

^a Absorption maximum.

gives evidence of the two fragments SF₅ and NO₂ being originally bonded together.

By gas density measurements, the molecular mass was determined to be 173 ± 0.5 g mol⁻¹ (calcd 173.1).

Gas-Phase Structure. The experimental radial-distribution curve was obtained by Fourier transformation of the molecular intensities, and it is relatively rich in structural information (Figure 7). This accounts for the fact that the experimental structure is well determined on the basis of electron diffraction data. As detailed in Table 3, just six geometric parameters were needed to define the molecular structure

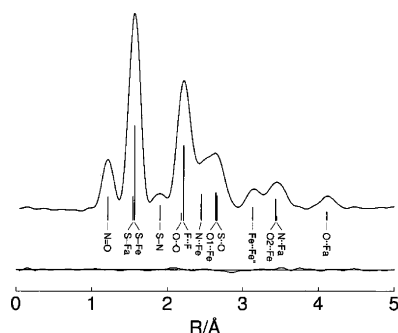


Figure 7. Experimental radial distribution function and difference curve. Interatomic distances are indicated by vertical bars. For atom numbering see Figure 8.

Table 3. Experimental and Calculated Geometric Parameters ($r/\text{\AA}$ or $\angle/^\circ$) for SF₅NO₂

	GED ^a	MP2/ 6-311++G(3df)	B3LYP/ 6-311++G(3df)
$r(\text{S}-\text{N})$	1.903(7)	1.895	1.979
$r(\text{S}-\text{F})_{\text{mean}}$	1.560(1)	1.571	1.588
$\Delta\text{SF} = (\text{S}-\text{F}_e) - (\text{S}-\text{F}_a)$	0.022(14)	0.019	0.026
$r(\text{S}-\text{F}_e)$	1.565(3)	1.575	1.593
$r(\text{S}-\text{F}_a)$	1.543(12)	1.556	1.567
$r(\text{N}=\text{O})$	1.209(3)	1.208	1.193
$\angle\text{F}_e-\text{S}-\text{F}_a$	90.8(2)	90.7	90.7
$\angle\text{S}-\text{N}=\text{O}$	115.4(5)	114.9	114.3
$\angle\text{O}=\text{N}=\text{O}$	129.2 (7)	130.3	131.3

^a r_{h1} values; uncertainties in parentheses are 3 σ values and refer to the last digit.

when the SF₅ group is constrained to C_{4v} symmetry. This constraint is justified by the ab initio calculations that predict a difference between the equatorial F–S–F bond angles of only 0.1°. In the final stage of the structural analysis, based on least-squares fitting of the molecular intensities, 10 vibrational amplitudes were refined simultaneously with these 6 geometric parameters. Only three correlation coefficients had values larger than |0.5|: SN/SNO = −0.68, $\Delta\text{SF}/2 = -0.76$, and $l6/l7 = -0.51$. The final results are listed in Table 3 (geometric parameters) and Table 4 (vibrational amplitudes) along with the calculated values.

The most striking feature of the SF₅NO₂ structure is an extremely long S–N bond of 1.903(7) Å. This bond is more than 0.2 Å longer than those in pentafluorosulfonyl amines, such as SF₅NF₂ (1.691(5) Å),³ (SF₅)₂NF (1.685(5) Å),^{19,20} and in the radical (SF₅)₂N• (1.692(4) Å).²¹ It is even longer than the S–N bond in the highly strained tris(pentafluorosulfonyl)-amine, (SF₅)₃N (1.829(6) Å).²¹ Considering the experimental

(19) Waterfeld, A.; Oberhammer, H.; Mews, R. *Angew. Chem. Suppl.* **1982**, 834.

(20) Waterfeld, A.; Oberhammer, H.; Mews, R. *Angew. Chem., Int. Ed. Engl.* **1982**, 21, 355.

(21) Weiss, I.; Thrasher, J. S.; Oberhammer, H. Unpublished work.

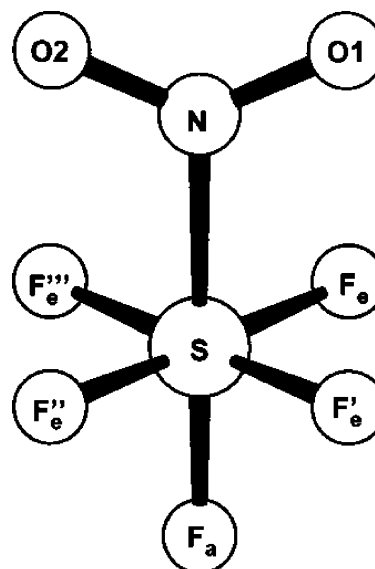
Table 4. Experimental Interatomic Distances and Experimental and Calculated Vibrational Amplitudes^a

	distance	amplitude GED		amplitude MP2/6-31G(d)
N=O	1.21	0.032(5)	<i>l</i> 1	0.037
S–F	1.54–1.56	0.044(2)	<i>l</i> 2	0.043
S–N	1.90	0.054(8)	<i>l</i> 3	0.059
O1–O2	2.18	0.047 ^b		0.047
F _e –F _e '	2.21	0.064(2)	<i>l</i> 4	0.066
F _a –F _e	2.21	0.064(2)	<i>l</i> 4	0.065
N–F _e	2.44	0.082(6)	<i>l</i> 5	0.081
O1–F _e	2.64	0.181(21)	<i>l</i> 6	0.134
S–O	2.65	0.068(8)	<i>l</i> 7	0.064
F _e –F _e ''	3.13	0.060(9)	<i>l</i> 8	0.054
O2–F _e	3.43	0.132(11)	<i>l</i> 9	0.109
N–F _a	3.44	0.066 ^b		0.066
O–F _a	4.11	0.084(15)	<i>l</i> 10	0.079

^a Values in Å; uncertainties in parentheses are 3 σ values and refer to the last digit. ^b Not refined.

error limit and the systematic difference between vibrationally averaged bond distances (r_{h1} values), derived in the experiment, and equilibrium bond distances (r_e values), derived with theoretical methods, the experimental S–N bond length is reproduced very well by the MP2 method with large basis sets (1.903(7) vs 1.895 Å). It is strongly overestimated, however, by the B3LYP method (1.979 Å). Calculated bond enthalpies depend strongly on the computational method, and values of 159 (MP2) and 87 kJ mol^{−1} (B3LYP) were derived. Because the B3LYP method overestimates the experimental S–N bond length strongly, we expect that this method underestimates the bond enthalpy and that the MP2 result (159 kJ mol^{−1}) is closer to the actual value.

It has been demonstrated that the mean S–F bond length in SF₅X compounds correlates with the electronegativity of X:²² that is, it decreases with increasing electronegativity. The mean S–F bond length in SF₅NO₂ (1.560(1) Å) is slightly shorter than that in SF₆ (1.5623(4) Å),²³ indicating the unexpected result that the NO₂ group is slightly more strongly electron withdrawing than fluorine. This can be rationalized by the strong π -donor ability of the fluorine atom

**Figure 8.** Molecular model with atom numbering.

in SF₅–F, which is absent in the –NO₂ group. This π back-bonding compensates for some of the electron withdrawing action of the fluorine atom. The axial S–F bond is shorter than the equatorial bonds by 0.022(14) Å. This result is in agreement with the *cis* influence predicted by Shustorovich and Buslaev for octahedral main group element compounds XEL₅.²⁴ According to this effect, the E–L bonds *cis* to X (equatorial bonds) are longer than the *trans* (axial) bond, when the E–X bond is more covalent than the E–L bonds. This influence is in contrast to that in transition metal compounds where the *trans* influence is well established. Both computational methods predict the mean S–F bond length to be slightly too long by 0.011 (MP2) and 0.028 Å (B3LYP).

Acknowledgment. We gratefully acknowledge the financial support of the Deutsche Forschungsgemeinschaft (DFG) and the Academy of Science of the Czech Republic (research plan AVOZ40320502). D.H. also thanks the DAAD for a travel grant.

IC0516212

(22) Zylka, P.; Mack, H.-G.; Schmuck, A.; Seppelt, K.; Oberhammer, H. *Inorg. Chem.* **1991**, 30, 59.

(23) Kelly, H. M.; Fink, M. *J. Chem. Phys.* **1982**, 77, 1813.

(24) Shustorovich, E. M.; Buslaev, Y. *Inorg. Chem.* **1976**, 15, 1142.